Earth and Planetary Science Letters 439 (2016) 48–57

Contents lists available at ScienceDirect

Earth and Planetary Science Letters

www.elsevier.com/locate/epsl

Role of arc magmatism and lower crustal foundering in controlling elevation history of the Nevadaplano and Colorado Plateau: A case study of pyroxenitic lower crust from central Arizona, USA

Monica E. Erdman *, Cin-Ty A. Lee, Alan Levander, Hehe Jiang

Dept. of Earth Science, Rice University, 6100 Main St. MS-126, Houston, TX 77005, USA

ARTICLE INFO

Article history:
Received 19 November 2015
Received in revised form 18 January 2016
Accepted 24 January 2016
Available online 3 February 2016
Editor: A. Yin

Keywords:
Colorado Plateau
Nevadaplano
uplift
delamination
cumulate
density inversion

ABSTRACT

Garnet–pyroxenite xenoliths from a 25 Ma volcano on the southern edge of the Colorado Plateau in central Arizona (USA) are shown here to have crystallized as deep-seated cumulates from hydrous arc magmas, requiring the generation of a large complement of felsic magmas. U–Pb dating of primary titanite grains indicates that crystallization probably occurred around 60 Ma. These observations suggest that voluminous arc magmatism reached as far inland as the edge of the Colorado Plateau during the Laramide orogeny. Here, we employ a combination of petrology, petrophysics, and seismic imaging to show that the formation and subsequent removal of a thick, dense, cumulate root beneath the ancient North American Nevadaplano modified the buoyancy of the orogenic plateau, possibly resulting in two uplift events. A late Cretaceous–early Tertiary uplift event should have occurred in conjunction with thickening of the crust by felsic magmatism. Additional uplift is predicted if the pyroxenite root later foundered, but such uplift must have occurred after ~25 Ma, the age of the xenolith host. We show that seismic velocity anomalies and seismic structures in the central part of the Colorado Plateau could represent pyroxenitic layers that still reside there. However, under the southern and western margins of the Colorado Plateau, the seismic signatures of a pyroxenite root are missing, despite xenolith records and geochemical evidence for their existence prior to 25 Ma. We suggest that these particular regions have undergone recent removal of the pyroxenite root, leading to late uplift of the plateau. In summary, our observations suggest that the Nevadaplano, west of the Colorado Plateau and now represented by the Basin and Range province, was underlain by high elevations in the late Cretaceous through early Tertiary due to magmatic thickening. This may have facilitated an east-directed drainage pattern at this time. Subsequent collapse of the Nevadaplano, culminating in Basin and Range extension and coupled with delamination-induced uplift of the margins of the Colorado Plateau in the late Cenozoic, may have reversed this drainage pattern, allowing rivers to flow west, as they do today.

© 2016 Elsevier B.V. All rights reserved.

1. Introduction

A combination of processes, including voluminous magmatism and tectonic thickening, leads to thickened crust in continental arc settings (Ducea et al., 2009; Lee et al., 2015). Such processes can lead to the development of large-scale, high-standing, low-relief plateaus. Ultimately, orogenic plateaus undergo extensional collapse due to their thickened crust, and the complex internal topographies that result from gravitational collapse provide insight into how continents are destroyed.

The ancient, exhumed North American Cordillera provides an excellent natural laboratory to study the construction and subsequent destruction of orogenic plateaus. Recent studies show that crustal thickening accompanied peak magmatism during the Late Cretaceous, contributing to an ancient high-elevation plateau, or Nevadaplano, in the hinterland of the Sevier orogenic belt (Cassel et al., 2014; Chapman et al., 2015; DeCelles, 2004; Henry et al., 2012; Paterson and Ducea, 2015). Magmatism ceased along the western margin of the continent and swept inland throughout the southwestern US during the Laramide orogeny, reaching as far inland as central Arizona, as indicated by the presence of Late Cretaceous–early Tertiary granites (Fig. 1B). In the magmatic lull that followed, crustal thinning and orogenic collapse began by Miocene time (Cassel et al., 2014; Chapman et al., 2015; Henry et al., 2012; Horton and Chamberlain, 2006). The resulting complex

* Corresponding author.
E-mail address: mee5@rice.edu (M.E. Erdman).

http://dx.doi.org/10.1016/j.epsl.2016.01.032
0012-821X/© 2016 Elsevier B.V. All rights reserved.

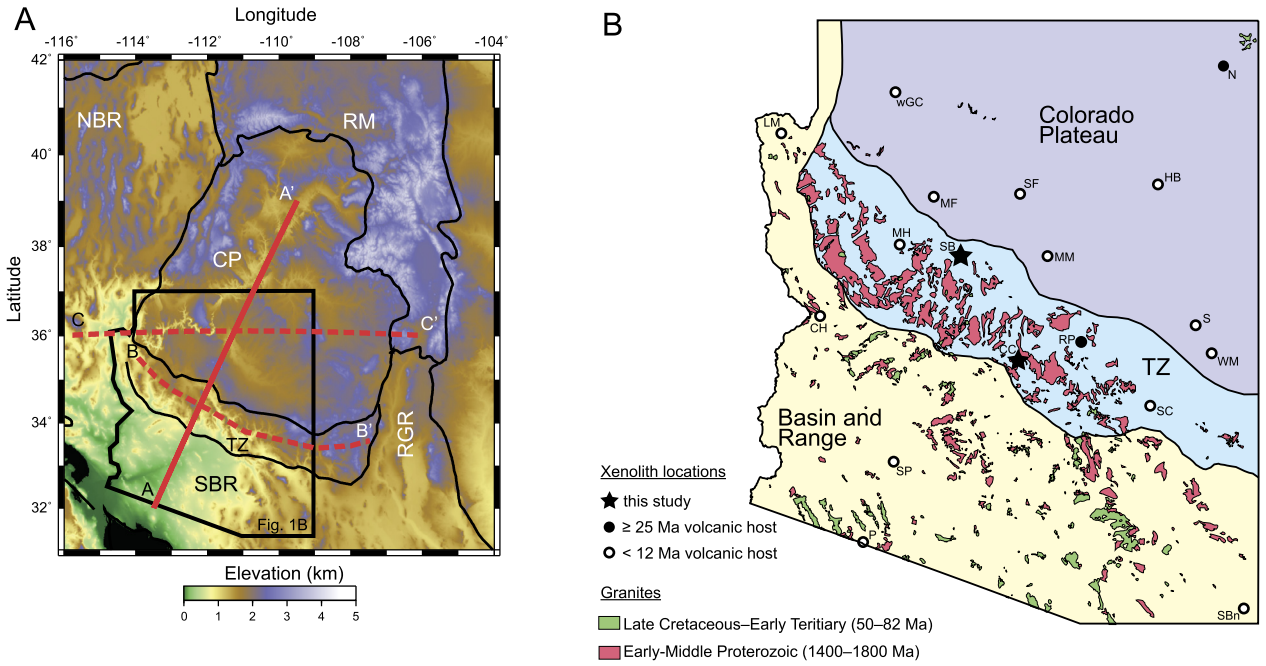

Fig. 1. Topography and simplified geologic map of the study region. (A) Topography of the Colorado Plateau and surrounding physiographic provinces (thin black lines). CP, Colorado Plateau; NBR, northern Basin and Range; SBR, southern Basin and Range; RGR, Rio Grande rift; RM, Rocky Mountains; TZ, Basin and Range–Colorado Plateau (BR-CP) Transition Zone. Profile AA' is the location of the seismic cross-sections in Fig. 4. Profiles BB' and CC' are shown in Supplementary Figs. 3–4. The thick black line outlines the map location in (B). (B) Simplified geologic map of Arizonan granite outcrops and sample locations (stars), modified from the Geologic Map of Arizona (Richard et al., 2002). Pastel colors shade the Colorado Plateau (purple), Basin and Range (yellow), and the BR-CP Transition Zone (blue) physiographic provinces. Other xenolith locations are marked by a circle, where closed circles mark volcanic hosts 25 Ma or older and open circles denote younger volcanic hosts. Garnet–pyroxenite xenoliths are conspicuously missing in young volcanic fields, which are dominated by mantle lithologies, such as spinel peridotite. Xenolith field locations are as follows: CC, Camp Creek; CH, Castaneda Hills; HB, Hopi Buttes; LM, Lake Mead; MF, Mount Floyd; MH, Mount Hope; MM, Mormon Mountain; N, Navajo; P, Pinacate; RP, Reno Pass; S, Springerville; SB, Sullivan Buttes; SBn, San Bernardino; SC, San Carlos; SF, San Francisco; SP, Sentinel Plains; wGC, western Grand Canyon; WM, White Mountains. (For interpretation of the references to color in this figure legend, the reader is referred to the web version of this article.)

topography of the North American Cordillera is exemplified by the relatively undeformed, low-relief Colorado Plateau within an otherwise highly deformed orogenic belt (Dickinson, 1989) (Fig. 1A). Marine sedimentary deposits atop the plateau suggest it was at or below sea level in the Late Cretaceous, but today rests 2 km above the surrounding regions. Free-air gravity indicates isostatic compensation across the Basin and Range and Colorado Plateau regions, yet the plateau's current crustal thickness of 40–50 km, especially along its edges, alone cannot support its elevation, requiring a sub-Moho component of buoyancy (Levander et al., 2011; Thompson and Zoback, 1979). Crustal thickness estimates vary considerably, approaching 55 km in some models, and suggest there is some complexity to the structure of the Colorado Plateau (e.g. Zandt et al., 1995).

Buoyancy gives rise to the Colorado Plateau's high elevations, yet how the buoyancy and elevation of the plateau evolved through time is unclear. Hypothesized explanations for epeirogenic uplift of the Colorado Plateau are varied and include: delamination of the Farallon plate following flat slab subduction (Bird, 1979; Humphreys, 1995), dynamic topography (Moucha et al., 2008), thermal expansion of the cold lithosphere after Farallon slab removal (Roy et al., 2009), mid-crustal flow from thickened crust (McQuarrie and Chase, 2000), and lithospheric foundering (Levander et al., 2011). Exactly when the plateau uplifted is also debated. Apatite U–Th/He thermochronometry studies from the Grand Canyon of northern Arizona yield conflicting results (Flowers, 2010), suggesting uplift occurred in the late Cretaceous (Flowers and Farley, 2012) or late Cenozoic (Karlstrom et al., 2014).

One way to assess paleo-elevations of a region is to examine the effect on nearby drainage systems. A recent thermochronometry study of surficial deposits on the southwestern Colorado Plateau presents evidence for two-stage incision of the Grand Canyon, and suggests the canyon was dominantly carved by an east-flowing river by 70 Ma followed by reversal of the river to flow westward in the Tertiary to excavate the final few hundred meters of the Grand Canyon (Flowers and Farley, 2012). Such dramatic hydrologic changes must have occurred in response to changes in topography, requiring high elevations in the west during the Cretaceous and collapse of the western highlands by Tertiary time.

Drivers of uplift are most likely sourced in the buoyancy of the crust, lithospheric mantle or asthenosphere. To gain insight into these deep sources of uplift, we integrate here new geochemical data and petrophysical calculations of lower crustal xenoliths with published seismic studies of the deep crust and upper mantle of the southwestern USA. Lower crustal xenoliths erupted within the 25 Ma Sullivan Buttes (Krieger et al., 1971) and similar-aged Camp Creek latites from the Basin and Range–Colorado Plateau Transition Zone (BR-CP TZ) in central Arizona provide a rare glimpse of the deep architecture of the plateau. The BR-CP TZ represents the transition between the thick crust of the stable, undeformed Colorado Plateau and the thin crust of the actively extending Basin and Range Province. The Arizonan lower crustal xenoliths are dominated by garnet–pyroxenite with minor amphibolite (Esperança et al., 1988). This mineralogy is compositionally denser than asthenospheric mantle (Lee, 2014; Lee et al., 2006), thus, their formation and removal could influence elevation. Pyroxenites also indicate a complementary volume of felsic magmas were emplaced into the crust. The low density of felsic magmas would contribute positive buoyancy to the continent. Here we show that magmatism influences elevation, via magmatic inflation of the crust and lower crustal foundering.

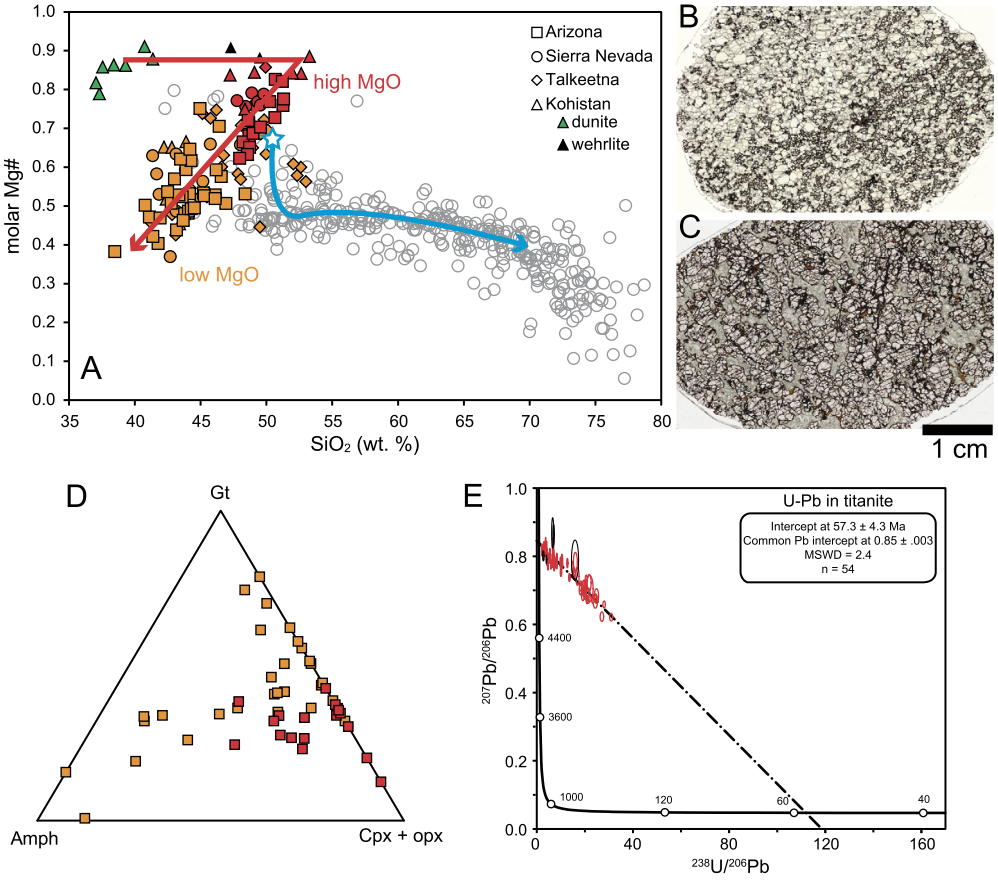

Fig. 2. Geochemistry and petrology of Arizonan cumulates. (A) Whole rock SiO_2 wt.% versus molar Mg# for rocks from the Colorado Plateau (squares; Supplementary Table 1), the Cretaceous Sierra Nevada continental arc (circles), Cretaceous Kohistan intraoceanic arc (triangles), and the Jurassic Talkeetna intraoceanic arc (diamonds). Samples from the Sierra Nevada, Kohistan, and Talkeetna arcs have a demonstrated cumulate origin. Red and orange symbols plot high MgO and low MgO cumulates, respectively. Open circles plot plutonic rocks from the Sierra Nevada batholith. Blue star represents a hypothetical primary mantle-derived arc basalt and the blue and red arrows show the inferred liquid and crystal lines of decent from this basalt, respectively. See Supplementary Data for full reference list. (B-C) Thin section scans of garnet-poor, high MgO (>13 wt. % MgO) pyroxenite (B) and garnet-rich, low MgO (<13 wt. % MgO) pyroxenite (C) from the Arizonan xenolith suite. The dull green minerals are clinopyroxene, the pale pink minerals are garnet, and the brown minerals in (C) are amphibole. Most of the opaque regions and garnet rims represent kelyphitic garnet breakdown products. (D) Modal abundance of dominant mineral phases in high vs. low MgO Arizonan xenoliths. Colors are the same as in (A). Apices plot at 100% of the phase(s) given. (E) Tera-Wasserberg Concordia plot of titanite U–Pb ages from four low MgO garnet–pyroxenites. All data uncertainties are reported at the 68.3% (1σ) confidence interval. Data points in black are excluded from the age calculation based on poor data quality during acquisition. Lower intercept represents a closure age; upper intercept represents the common Pb component. (For interpretation of the references to color in this figure legend, the reader is referred to the web version of this article.)

2. Analytical methods

Whole-rock major element compositions were measured via X-ray fluorescence spectroscopy (XRF) at the University of Washington at Pullman. To prepare samples for XRF analysis, fresh sample sizes of 10–100 g were crushed and powdered in a ceramic SPEX mill placed in a shatterbox for 5–10 minutes per sample. Major element concentrations of minerals were acquired in wavelength-dispersive spectroscopy mode on the Cameca SX 50 microprobe at Texas A&M in College Station, TX. Spot size was 10 µm. Garnet, clinopyroxene, orthopyroxene, and amphibole standards were used for external calibration. *In-situ* U–Pb titanite ages were determined at Rice University on a single-collector, magnetic sector ICP-MS (ThermoFinnigan Element 2) coupled to a New Wave 213 nm laser ablation system (10 J/cm^2 laser fluence, 10 Hz repetition rate, 30 µm spot size). Titanite standards FCT and BLR were used to monitor accuracy and zircon standard 91500 was used as an external standard. Detailed methods are described in Jiang et al. (2015).

3. Arizonan garnet–pyroxenite petrogenesis

3.1. Petrology and geochemistry

Geochemical and petrologic observations allow for the separation of the Arizonan garnet–pyroxenites into two groups: 1) a high MgO, low Al_2O_3, and high clinopyroxene mode (>50 vol.%) group ($n = 16$), characterized by a fine-grained, equigranular texture with 120° triple junctions and 2) a low MgO, high Al_2O_3, and high garnet ± amphibole mode group ($n = 32$), characterized by coarse-grained, poikilitic texture (Fig. 2). The textures of the high MgO group are indicative of partial to complete metamorphic recrystallization and the textures of the low MgO group indicate an igneous cumulate origin.

Major element signatures of both pyroxenite groups overlap with lower crustal cumulates from mature magmatic arc systems, such as the Sierra Nevada continental arc, and the Kohistan and Talkeetna intraoceanic arcs (Fig. 2A). Magmatic differentiation of primitive arc basalt (blue star), as exemplified by the trend of mafic to felsic plutonic rocks from the Sierra Nevada batholith, shows an initial decrease in Mg# (molar Mg/(Mg + Fe_T), where Fe_T is total Fe) at constant SiO_2, followed by an increase in SiO_2 at relatively constant Mg# (blue line in Fig. 2A). This liquid line of descent can be explained by crystallization of high MgO pyroxenites early in the differentiation trend, dropping the Mg# of the melts, followed by crystallization of low MgO pyroxenites, to increase the SiO_2 content of the melts (Lee, 2014; Lee et al., 2006). The compositional similarity of the Arizonan pyroxenites with known magmatic cumulates, combined with relict cumulate textures in the low MgO pyroxenites, suggests the Ari-

zonan pyroxenites are also arc cumulates. Thus, the high MgO pyroxenites represent primitive cumulates and the low MgO pyroxenites represent cumulates from more evolved intermediate magmas. A primary cumulate origin is consistent with experimental studies showing garnet and clinopyroxene on the liquidus of primitive arc melts in deep crustal settings (Alonso-Perez et al., 2008; Müntener et al., 2001).

3.2. Temperature and pressure estimates

Mineral compositions were measured in 13 samples (Supplementary Table 1). Garnet–clinopyroxene Fe–Mg exchange thermometry (Ellis and Green, 1979; Krogh, 1988; Krogh-Ravna, 2000) performed on 12 samples from both cumulate groups indicate final equilibration temperatures of ~650–800 °C or lower (calculated at 2 GPa), suggesting the whole lower crustal root cooled considerably after magmatism ceased. A single orthopyroxene-bearing sample gives estimates of both temperature and pressure via the Ca-in-opx thermometer and Al-in-opx barometer (Brey and Köhler, 1990), and suggests equilibration pressures of 2.3–2.8 GPa (70–85 km), in agreement with Smith et al. (1994). These results indicate emplacement well below typical Moho depths. The partially to completely recrystallized textures of the high MgO pyroxenites suggest slow cooling from magmatic temperatures, providing time for textural recrystallization. Slow cooling is expected at sub-Moho depths where ambient temperatures are high. In contrast, preservation of the original cumulate textures in low MgO pyroxenites indicates no significant subsolidus recrystallization, suggesting these rocks cooled quickly and thus at shallow depths where ambient temperatures are cooler (20–35 km). Unfortunately, the low MgO pyroxenites do not have appropriate mineral assemblages for barometry, but the presence of amphibolites within this group is consistent with a lower pressure origin (Alonso-Perez et al., 2008). Thus, these observations suggest lower crustal roots are comprised of two compositional layers, with more evolved, low MgO cumulates above deeper-seated, primitive, high MgO cumulates.

3.3. Age constraints

Several low MgO pyroxenites contain anhedral, coarse-grained titanite. Combined with the cumulate textures of the garnets and pyroxene grains, the titanites probably also grew as a primary cumulate phase. If this is the case, titanite ages can be used to constrain the time of cumulate formation. Using methods developed at Rice University (Jiang et al., 2015), we determined an *in-situ* titanite U–Pb age of 57.3 ± 4.3 Ma from four low MgO pyroxenites (Fig. 2E). Titanite in one of the four samples dated has rutile cores, suggesting initial crystallization at either higher pressures or under oxidized conditions (Frost et al., 2000). Despite coarse grain sizes, titanite shows little zoning and laser ablation spots from both rims and cores yield concordant ages, suggesting rapid cooling in these samples to below the closure temperature of titanite (~650–700 °C, Frost et al. (2000)).

Previous isotopic age determinations for the Arizonan pyroxenites have yielded diverse and complex results. Whole rock Sr, Nd, and Pb isotopic systematics give imprecise ages suggesting formation in the Proterozoic (Esperança et al., 1988), coincident with the age of the basement in this area (Wendlandt et al., 1993). Others have proposed instead that the xenoliths formed during Phanerozoic basaltic underplating (Johnson, 1990). In contrast, mineral Rb–Sr and Sm–Nd internal isochrons yield young ages identical within uncertainty to the age of eruption of the host latite (Esperança et al., 1988). Titanite U–Pb ages reported here support recent crystallization of the pyroxenites. The apparent Proterozoic whole-rock Sr, Nd and Pb ages could instead reflect mixing ages between juvenile and ancient components in the deep crustal magma chambers that gave rise to the pyroxenite cumulates.

4. Petrophysical properties

4.1. Density

To quantify the buoyancy of a lower crustal root comprised of the Arizonan pyroxenites, we calculate densities for these compositions. Results are shown (yellow symbols, Supplementary Fig. 2A) for 12 pyroxenites with low amphibole mode at STP (298 K, 1 bar) conditions calculated from measured mineral compositions and modal abundance (Hacker and Abers, 2004) (Supplementary Tables 1–2). Modal proportions were determined via point counting of thin sections. Density for these samples varies linearly with bulk Mg# for samples with low amphibole content (<30 vol.%). This empirical relationship allows extrapolation of densities for the remaining samples for which bulk rock chemistry and mineral modes are known but mineral compositions were not measured. We thus extrapolate for the remaining 43 samples according to the linear regression shown in Supplementary Fig. 2A (blue symbols). Because amphibole has significantly lower density than garnet or clinopyroxene, this must be accounted for in amphibole-rich samples (>30 vol.%). For these samples ($n = 9$), we calculate density as the weighted average between pure hornblende (Hacker and Abers, 2004) and the estimate from the linear regression according to the modal proportions of amphibole and garnet + clinopyroxene, respectively (green symbols).

Nearly all compositional densities for the Arizonan pyroxenites are greater than peridotitic upper mantle (3.378 g/cm^3 at STP (Lee, 2003)); only those with high amphibole mode are equal to or lower, but these represent a minority. On average, compositional densities are 6% denser than fertile peridotite. Accounting for thermal contraction due to cooling of the pyroxenites below 700 °C increases the density contrast between the mafic root and the hot (~1400 °C) ambient mantle by an additional 2%. Fig. 3C shows the resulting densities vary from 2 to 17% denser than peridotite (8% on average). Such high density inversions are not expected to persist long without convective recycling of the garnet–pyroxenite root into the mantle (Lee, 2014).

4.2. Elastic moduli and seismic velocities

To evaluate whether a pyroxenite root persists today beneath the former orogenic plateau, we calculate the elastic moduli and seismic velocities of the Arizonan pyroxenites (Supplementary Figs. 1–2) and compare to existing seismic studies in the region. As with density, the elastic moduli of rocks can be calculated from mineral chemistry and their modal proportions. These values also vary linearly with bulk Mg# (Supplementary Fig. 1), and similar to the density calculations, we extrapolate via linear regression for the samples with unknown mineral compositions. For amphibole-rich samples, we calculate the elastic moduli as the Voigt–Reuss–Hill average between pure hornblende and the linear regressions in Supplementary Fig. 1 according to the modal proportions of amphibole and garnet + clinopyroxene. For comparison with seismic images, V_P and V_S were calculated for all samples from the density and elastic moduli determinations. Because density and seismic velocity are determined for standard temperature and pressure (298 K, 1 bar) conditions, direct comparison with seismic tomography observations requires projection to higher temperature and pressure. We calculate density and seismic velocities for the 13 samples with known mineral compositions at 700 °C via the method of Hacker and Abers (2004). Assuming a linear relationship between 25 and 700 °C for each, we take the

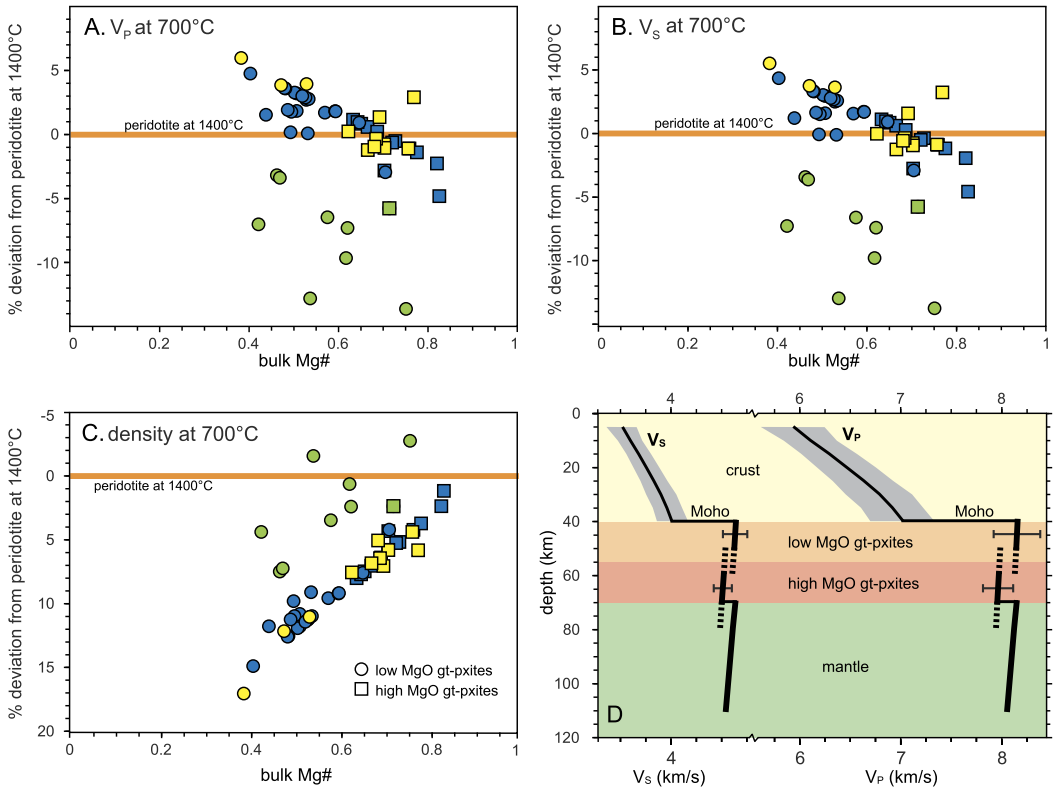

Fig. 3. Calculated geophysical properties of the Arizonan xenoliths. Density (A), V_P (B), and V_S (C) versus bulk Mg# for high MgO garnet–pyroxenites (squares) and low MgO garnet–pyroxenites (circles) at 700 °C plotted as a percent difference from convecting mantle peridotite (Lee, 2003) at 1400 °C (orange bar). Note inverse y-axis scale for density plot (A). These values are meant to compare directly with seismic observations. Yellow symbols indicate samples with measured mineral compositions whose geophysical properties are determined using the method of Hacker and Abers (2004). Samples whose physical properties are calculated based on the linear regressions for Mg# versus bulk modulus, shear modulus, and density (Supplementary Figs. 1–2) are plotted in blue. Green symbols show amphibole-rich samples; error bars show the uncertainty due to the high amphibole content in these samples. (D) Schematic 1-D P- and S-wave velocity versus depth profile calculated for a 55 mW/m^2 geothermal gradient. Error bars on garnet–pyroxenite velocities represent compositional variation. Velocity is dashed where boundaries between layers are uncertain. Crustal velocities are from Christensen and Mooney (1995). (For interpretation of the references to color in this figure legend, the reader is referred to the web version of this article.)

slope of the line connecting the two points as equal to $\frac{d\rho}{dT}$, $\frac{dV_P}{dT}$, and $\frac{dV_S}{dT}$. We then use the slope to project the density and seismic velocities of the remaining samples and peridotite to high temperature. Because we report density and velocity relative to peridotite at the same pressure, the effect of pressure on these values are similar and are thus ignored.

V_P and V_S perturbation of cold (700 °C) pyroxenites relative to hot asthenosphere (1400 °C) decrease with increasing Mg#, such that low MgO pyroxenites are faster and high MgO pyroxenites are slower than asthenospheric mantle (Fig. 3A–B). Thus, a complex velocity profile is predicted for a stratified lower crustal root comprised of low MgO pyroxenites above and high MgO pyroxenites at the base. With increasing depth, the transition from felsic crust to low MgO pyroxenites corresponds to a velocity increase (i.e., the Moho), followed by a velocity decrease at the transition from the shallow low MgO pyroxenites to the deeper high MgO pyroxenites, and a final velocity increase where high MgO pyroxenites transition to peridotitic mantle (Fig. 3D). Thus, unique seismic signals likely exist in regions where mafic lower crustal roots are present. In the case of teleseismic receiver functions, we predict two positive events with a negative event in between, generating a "double Moho" signature.

5. Comparison with seismic sections

We use PdS and SdP receiver functions and Rayleigh wave tomography to reveal the sub-surface structure beneath the Colorado Plateau region (Levander et al., 2011). The processing to construct the seismic images is described elsewhere (Levander and Miller, 2012; Levander et al., 2011; Liu et al., 2011). All of the seismic data were recorded by the USArray component of EarthScope, a seismic array with a nominal ~70 km instrument spacing. A receiver function (RF) is a time series in which the earthquake source function has been removed and replaced with a known shaping function to identify scattered waves. Receiver function images depict continuous interfaces, such as the Moho, that have large impedance contrasts in elastic properties. RF signals can also arise from less vertically abrupt elastic parameter changes such as the lithosphere–asthenosphere boundary (LAB), depending on the frequency content of the signal. The RFs have been processed to make scattered wave images of the subsurface using P to S (PdS) or S to P (SdP) converted waves from teleseismic earthquake signals, using a technique referred to as common conversion point (CCP) stacking (Dueker and Sheehan, 1997). In CCP stacking an assumed velocity model is used to convert receiver functions from a seismic array to depth and reposition them laterally to the point where the input P (or S) wave encountered an impedance contrast to produce a converted S (or P) wave. Summing partial images made from many earthquakes, referred to as stacking, improves signal to noise ratio in the image. In contrast, finite-frequency Rayleigh wave tomography provides a measurement of the absolute isotropic shear velocity at different depths of the earth, with sampling depth and resolution depending on frequency. The Rayleigh waves used in this study (0.0167–0.05 Hz) are sensitive to V_S structure from the mid-crust, ~15–20 km, into the upper mantle, ~150–200 km depth, with resolution adequate for distinguishing between crustal, lithospheric mantle, and asthenospheric mantle structure.

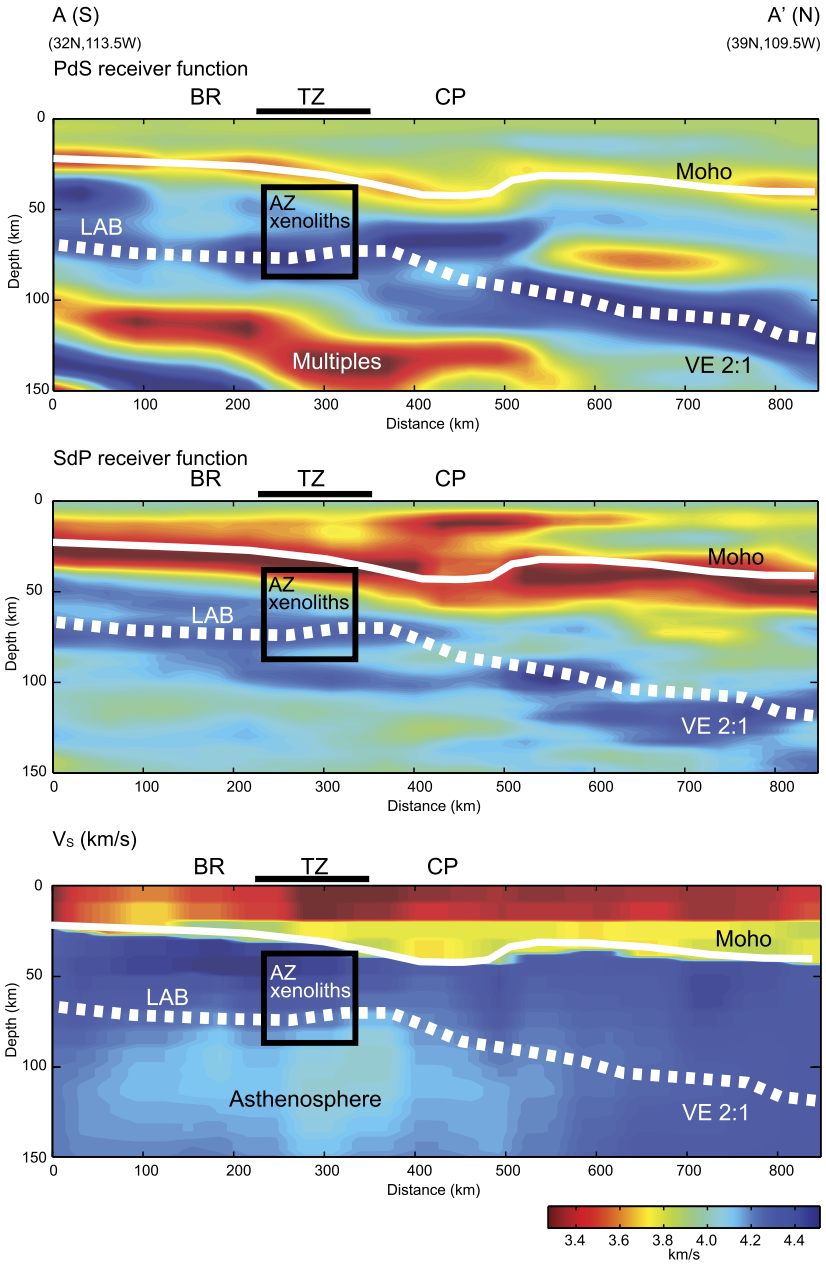

Fig. 4. Seismic profile across the Basin and Range and Colorado Plateau. PdS and SdP receiver function and Rayleigh wave tomography shear wave velocity cross-sections along AA'. Solid white line is the Moho; dashed white line is the LAB. Black box shows the approximate source location of the Arizonan garnet–pyroxenite xenoliths as determined by thermobarometry (this study and Smith et al., 1994). A "double Moho" feature is present in the PdS and SdP receiver function images between $x = 550$–750 km beneath the northern Colorado Plateau (also see Supplementary Fig. 4). This unique signal suggests an intact stratified garnet–pyroxenite lower crustal layer, likely already foundering (Levander et al., 2011). LAB depth is greatest underneath the "double Moho" event (>110 km) in the north, and shallows to <80 km beneath the BR-CP-TZ and Basin and Range. Rayleigh wave tomography reveals a low velocity zone beneath the southern Colorado Plateau, BR-CP-TZ, and Basin and Range, suggesting upwelling asthenosphere in this region. (For interpretation of the colors in this figure, the reader is referred to the web version of this article.)

Profile AA', shown in Fig. 4, crosses the xenolith locations, extending from the Southern Basin and Range Province in the south to the northern part of the Colorado Plateau (see Fig. 1A). Beneath the BR-CP-TZ, where we may expect to see a "double Moho" feature based on the presence of garnet–pyroxenite xenoliths, no such structure can be seen in the seismic profile. However, on the PdS receiver function image, a "double Moho" feature is clearly visible in the central part of the plateau 550–750 km from point A. Based on our predicted 1-D seismic profile in Fig. 3D, this observation suggests that a cumulate lower crustal root is present beneath the central Colorado Plateau. Yet, the lack of geologic evidence for magmatic thickening, such as granitic plutonism, across the plateau makes it difficult to interpret the seismic feature in this manner. Nevertheless, the seismic profile indicates a layer with high impedance contrast is present within the central Colorado Plateau lithosphere, but is absent to the south. Profile BB' parallels the BR-CP-TZ and shows uniform Moho and LAB depths across this distance, indicating similar processes modified the entire BR-CP-TZ (Supplementary Fig. 3). Receiver function images in Fig. 4 show the LAB shoals from >110 km in the north to <80 km beneath the southern half of the plateau and BR-CP-TZ, with a corresponding shallowing of the Moho towards the Basin and Range. Similar conclusions can be drawn from profile CC', where a "double Moho" signature correlates with thickened lithosphere beneath the eastern Colorado Plateau and disappears to the west (Supplementary Fig. 4).

6. Implications for the topographic evolution of the North American Cordillera

High Sr/Y ratios in magmatic rocks from the hinterland of the Sevier fold and thrust belt in the southwestern US suggests garnet- and/or amphibole-bearing cumulates crystallized from these magmas in the lower crust of the former Nevadaplano, which lay just west of the present Colorado Plateau in the current-day Basin and Range Province (Chapman et al., 2015). Our garnet–pyroxenitic xenoliths confirm this inference. If titanite is a primary cumulate phase in these rocks, U–Pb titanite ages suggest cumulates formed in the BR-CP-TZ no later than 60 Ma. This age is consistent with the interpretation that the Arizona pyroxenites may be the mafic complements to the Late Cretaceous–early Tertiary granites that were emplaced through much of the American southwest during the beginning of the Laramide orogeny. Most of the magmatism occurs west of the plateau, but if the garnet–pyroxenites are petrogenetically related to these young granitoids, their presence on the western edge of the plateau suggests that arc magmatism may have extended into the western and southern Colorado Plateau regions in Late Cretaceous–early Tertiary times. As we will discuss later, voluminous magmatism during the Late Cretaceous–early Tertiary across southwestern USA may have thickened the upper crust significantly, while simultaneously generating a thick, dense cumulate lower crustal root (Chapman et al., 2015), and contributing to the high elevations of the Nevadaplano (Cassel et al., 2014; DeCelles, 2004; Ducea et al., 2015; Henry et al., 2012). The eruption of the xenolith host lava at 25 Ma indicates this cumulate root was in place for at least 35 Myr after its formation around 60 Ma. The seismic observations presented in Section 5, however, suggest pyroxenite roots are now absent beneath the Basin and Range, western Colorado Plateau, and BR-CP TZ.

Recent removal of the garnet–pyroxenite cumulate root may explain these interpretations. The “double Moho” feature beneath the northern Colorado Plateau (profile AA’) is positioned at the eastern edge of a fast P-wave anomaly extending to 200 km depth, which has been interpreted as an active lithospheric downwelling (Levander et al., 2011). Recent removal of the pyroxenite root is consistent with the fact that younger ($\leq$12 Ma) basaltic eruptions in the region contain xenoliths reflecting mantle lithologies, such as spinel peridotite, but no garnet–pyroxenites, as is characteristic of older xenolith localities (Nealy and Sheridan, 1989) (Fig. 1B). Rayleigh wave V_S tomography across profile AA’ reveals a low velocity zone beneath the shallow LAB along the plateau’s southern margin, which may represent upwelling asthenospheric mantle that replaced the foundered material. Spatio-temporal patterns of magmatism show magmatic activity migrating inward from the plateau margins during the mid-Cenozoic (Crow et al., 2010; Reid et al., 2012; Roy et al., 2009), which may be a manifestation of progressive inward foundering of the pyroxenite root. In addition, geomorphic constraints from Colorado River incision rates suggest increased deep-seated buoyancy has been propagating toward the interior of the Colorado Plateau at least over the last 4 Ma (Crow et al., 2014).

The geophysical, petrologic and geologic data presented here collectively suggest that during the Late Cretaceous–early Tertiary, the present-day Basin and Range and BR-CP TZ was thickened by the influx of arc magmas, generating a package of buoyant felsic crust and a dense cumulate root. This cumulate root persisted at least until 25 Ma in the BR-CP TZ and subsequently foundered to be replaced by hot asthenospheric mantle. This sequence of events must have influenced surface elevations. The isostatic response of elevation (Δh) to density changes depends linearly on the change in crustal thickness (ΔH) and the effective density difference between the crustal column of interest and the background reference state. That is, $\Delta H = (1 - \frac{\rho_x}{\rho_m})\Delta h$, where ρ_m and ρ_x are the density of the mantle and the modified crust. During magmatic inflation, low-density felsic magmas increase buoyancy, but the accumulation of dense mafic cumulates decreases buoyancy. Hence, the ratio of mafic to felsic magmatic additions (M:F) ultimately determines the isostatic response (Fig. 5A). Geochemical mass balance in arc sections indicates that $\sim$70% of magmatic additions are mafic cumulates (Lee, 2014), which we use here as a maximum M:F value at any given time within the crustal section. Retention of the entire cumulate package (high M:F) with the felsic crust results in only a modest elevation increase ($<$1 km). If, instead, some cumulates are immediately recycled into the mantle during magmatism (low M:F), uplift associated with felsic crust generation may be more significant. Estimates suggest the upper crust of the Nevadaplano magmatically thickened by 25 km in the Late Cretaceous (Chapman et al., 2015), implying growth of a thick, garnet–pyroxenite root at the base of the orogenic plateau. Depending on the thickness of cumulates retained in the lower crust, isostasy predicts the Nevadaplano may have increased in elevation by 1.5–2 km (for M:F = 1; Fig. 5A), in agreement with eastward flowing drainage systems at this time (Flowers and Farley, 2012). The density inversion formed by the growth of a thick, dense cumulate root at the base of the crust, however, leads to lower crustal foundering. Another possibility is that cumulates were removed via melting, perhaps contributing to the ignimbrite flare-up of the southwestern US (Lipman, 1992). The combination of secular change in xenolith demographics and seismic evidence for lithospheric thinning across the Basin and Range and southern perimeter of the Colorado Plateau (Figs. 1B and 4) provide indirect evidence for cumulate removal. Isostatic equilibrations following lower crustal foundering could double elevation increases across this area, assuming removal of a 25 km-thick root with density 6% greater than peridotite (Fig. 5B). In detail, there are a number of factors, such as sedimentation and heterogeneous crustal roots, which we do not consider in this simple calculation, but such considerations will not change the fact that removal of a dense, pyroxenitic root results in significant uplift.

The simple calculations shown in Figs. 5A and 5B imply that two episodes of uplift likely affected the southwestern US, one during magmatic inflation of the Nevadaplano and a second uplift event caused by lower crustal foundering. The first uplift event probably occurred in the Late Cretaceous–early Tertiary, as constrained by U–Pb titanite age dating of pyroxenite cumulates (Section 3.3) and the age of magmatism across the former Nevadaplano. The timing of the second uplift event is difficult to measure, as it relies on the removal of material for which we do not have a definite constraint in terms of timing. The age of the host lavas that erupted the Arizona pyroxenite xenoliths constrains uplift to have occurred after 25 Ma. Paleo-altimetry and thermochronology studies provide additional constraints on the age of uplift. U–Th/He thermochronology (Flowers and Farley, 2012) and carbonate clumped isotope thermometry (Huntington et al., 2010) of the southwestern Colorado Plateau suggest significant unroofing began in the Late Cretaceous ($\sim$70–60 Ma). In contrast, apatite fission track dating combined with U–Th/He thermochronometry (Karlstrom et al., 2014), basalt vesicularity paleoaltimetry (Sahagian et al., 2002), and U–Pb dating of speleothems (Polyak et al., 2008) from the same study area suggest major uplift may be significantly younger. These apparently conflicting findings are consistent with the two-stage uplift history proposed in this study.

7. Enigmatic Colorado Plateau elevations

That the Colorado Plateau sits at high elevation yet seismically appears to retain a cumulate root beneath its center must be addressed. We consider two scenarios to explain the current high elevations of the Colorado Plateau. The first scenario is that the cu-

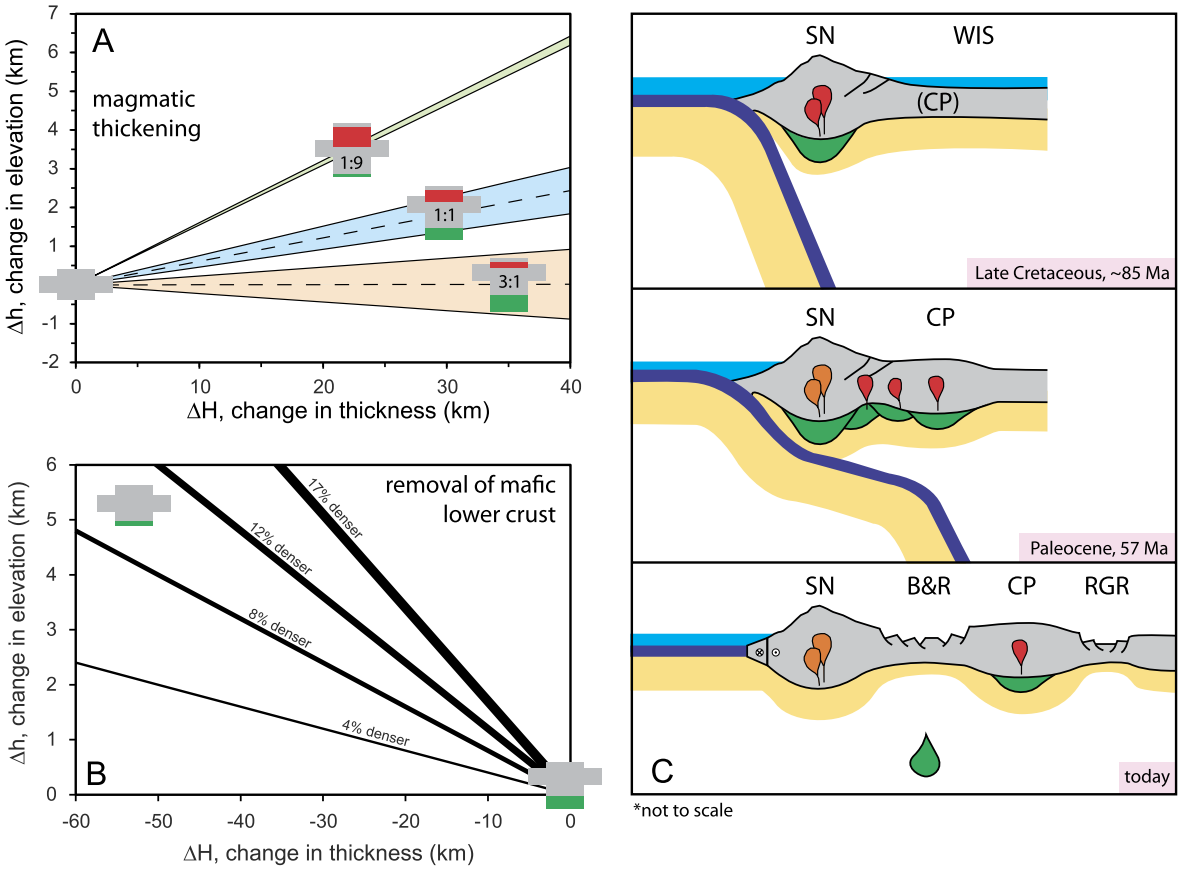

Fig. 5. Model for the evolution of the former Nevadaplano. (A) The isostatic response to magmatic thickening for three different ratios of mafic cumulates to felsic magma additions; M:F ratio is given. For each ratio considered, the colored region shows the 1 std. dev. variation in compositional density difference from the average for the cumulate root (6% denser than the mantle; dashed lines). Felsic magmas are assumed to have a density equal to the surrounding crust. (B) Removal of a cold and dense lower crustal root results in isostatic uplift; various density contrasts are considered. (C) Schematic model for the evolution of the western US margin at the latitude of the BR-CP-TZ. B&R, Basin and Range; CP, Colorado Plateau; RGR, Rio Grande Rift; SN, Sierra Nevada; WIS, Western Interior Seaway. In the Late Cretaceous, the Cordilleran magmatic front was located in the Sierra Nevada and the proto-Colorado Plateau was at sea level beneath the Western Interior Seaway. By Paleocene times, magmatic volcanism had swept toward the interior of the continent during Farallon Plate flat-slab subduction, resulting in magmatic inflation and development of a thick and dense, garnet-pyroxenitic lower crustal root. Elevation gain due to magmatic thickening likely occurred at this time. Subsequent foundering of the dense lower crust beneath the Basin and Range, BR-CP-TZ after 25 Ma, as well as beneath the Sierra Nevada in the Late Cenozoic (Ducea and Saleeby, 1996; Wernicke et al., 1996), isostatically uplifted these regions. Partial removal of a pyroxenitic root also likely occurred beneath the Colorado Plateau to uplift this region to its current elevation. The associated influx of hot asthenospheric mantle with the removal of the lower crust likely acted to thermally weaken and convectively thin Basin and Range crust, ultimately causing an isostatic response to subside the region to its current elevation. Thermal relaxation beneath the Colorado Plateau and Sierra Nevada will, in the future, act to decrease elevations to a new isostatic equilibrium elevation.

mulate root formed in place during magmatic thickening and uplift occurred via removal of the lower crust. Geologic evidence for felsic magmas on the Colorado Plateau, however, is minimal (Fig. 1B). If magmas were emplaced intrusively rather than extrusively, low erosion rates may explain the lack of surficial exposure of granites or their extrusive equivalents on the plateau. *Partial* lower crustal foundering may explain why the central Colorado Plateau retains a "double Moho" feature at its base. Removal of a 25 km-thick layer of high MgO cumulates from the lower crust is adequate to explain the current elevation of the Colorado Plateau, assuming it is 6% denser than the mantle (Fig. 5B). If the plateau was already at higher elevations due to isostatic equilibration during magmatic thickening, removal of a smaller portion of the cumulate root is sufficient to explain the plateau's present-day elevation.

An alternative scenario is to consider the possibility that the cumulate root did not form in place, but instead was tectonically translated to its current position, presumably from the west. Studies have proposed that during flat slab subduction of the Farallon Plate, material was tectonically eroded from the forearc and transported inland to be incorporated into the lithosphere, possibly reaching as far east as the Colorado Plateau (Luffi et al., 2009; Saleeby, 2003; Smith, 2013). If cumulates formed beneath the Sierra Nevada arc in California were translated eastward to the Colorado Plateau, this could explain the apparent lack of complementary felsic rocks on the plateau. However, the fact that many of the Arizona xenoliths retain their igneous cumulate textures suggests that they did not undergo significant deformation, which might be expected during tectonic erosion and translation in the mantle wedge. Additionally, this scenario predicts a very different uplift history than the first. Translation of a dense cumulate root eastward to the base of the Colorado Plateau would cause subsidence if it is not accompanied by emplacement of buoyant, felsic upper crust. As with the first scenario, this situation also requires only partial removal of the lower crustal root to explain the plateau's current high elevations while retaining a "double Moho" seismic signature. However, the thickness of cumulates removed must be greater (than required in the first scenario) in order to transition from the low elevations achieved during cumulate translation, and associated isostatic subsidence, to 2 km above sea level today. Paleo-altimetry and thermochronology studies do not support subsidence prior to uplift of the Colorado Plateau (Flowers and Farley, 2012; Huntington et al., 2010; Karlstrom et al., 2014; Polyak et al., 2008; Sahagian et al., 2002). The two scenarios discussed here are possible explanations for the observed seismic

impedance contrast below the Moho of the Colorado Plateau. Conclusive interpretation of the "double Moho" structure is difficult at this time; however, the Arizonan xenoliths provide an additional piece of evidence to coax the story from the geologic record.

8. Conclusions

In summary, we use a combination of geochemistry, petrology, petrophysics, and geophysics to understand how the topography of the southwestern US has evolved through time. We report the occurrence of garnet–pyroxenite cumulates in the BR-CP-TZ, suggesting voluminous magmatism reached as far inland as central Arizona during the Laramide orogeny. Magmatic inflation and growth of a cumulate root acted to raise elevations across the Nevadaplano during this time. After magmatism ceased, the density inversion created during cooling of the crust and lithosphere led to lower crustal foundering in the Miocene or younger, resulting in a second uplift event. If our model is correct, a two-stage uplift history is predicted to accompany all regions affected by voluminous magmatism, especially if such magmatism differentiates into felsic upper crust and mafic pyroxenitic lower crust. In fact, a similar model is employed to explain the high elevations of the southern Sierra Nevada despite thin supporting crust and mantle lithosphere (Ducea and Saleeby, 1996; Wernicke et al., 1996). Evidence of uplift, however, may not always be preserved, as post-foundering thermal relaxation will cause the thermal boundary layer to cool and thicken, causing high elevations to eventually subside.

Foundering of a cumulate root exposes the remaining upper crust to upwelling, hot asthenosphere, which could lead to melt infiltration and weakening of the crust, priming it for further crustal thinning. This may explain the differential deformation between the actively deforming Basin and Range Province and the tectonically stable Colorado Plateau. That a pyroxenite root appears to persist beneath the Colorado Plateau's interior in combination with a thick lithospheric mantle, suggests the crust is protected from the deep convecting mantle. However, active foundering beneath the western Colorado Plateau (Levander et al., 2011) may, in the future, destabilize the plateau's long history of tectonic quiescence. Precise determination of the uplift/subsidence history of the southwestern US will aid in understanding the temporal differences in deep crustal thinning between the Basin and Range and Colorado Plateau regions, as proposed in this study.

Acknowledgements

Thank you to Doug Smith for providing a subset of the xenolith samples. EPMA data was collected with the invaluable assistance of Ray Guillemette at Texas A&M, College Station, TX. We thank Alan Chapman and Brad Hacker for insightful comments on our ideas. This paper benefited from reviews by Mihai Ducea and an anonymous reviewer. Constructive reviews from Doug Smith, Esteban Gazel, and two anonymous reviewers helped to improve an earlier version of the manuscript. This work was supported by NSF Grant EAR-13470850 awarded to Lee.

Appendix A. Supplementary material

Supplementary material related to this article can be found online at http://dx.doi.org/10.1016/j.epsl.2016.01.032.

References

Alonso-Perez, R., Müntener, O., Ulmer, P., 2008. Igneous garnet and amphibole fractionation in the roots of island arcs: experimental constraints on andesitic liquids. Contrib. Mineral. Petrol. 157, 541–558.

Bird, P., 1979. Continental delamination and the Colorado Plateau. J. Geophys. Res. 84, 7561–7571.

Brey, G.P., Köhler, T., 1990. Geothermobarometry in four-phase lherzolites II. New thermobarometers, and practical assessment of existing thermobarometers. J. Petrol. 31, 1353–1378.

Cassel, E.J., Breecker, D.O., Henry, C.D., Larson, T.E., Stockli, D.F., 2014. Profile of a paleo-orogen: high topography across the present-day Basin and Range from 40 to 23 Ma. Geology 42, 1007–1010.

Chapman, J.B., Ducea, M.N., Decelles, P.G., Profeta, L., 2015. Tracking changes in crustal thickness during orogenic evolution with Sr/Y: an example from the North American Cordillera. Geology 43, 919–922.

Christensen, N.I., Mooney, W.D., 1995. Seismic velocity structure and composition of the continental crust: a global view. J. Geophys. Res. 100, 9761–9788.

Crow, R., Karlstrom, K., Asmerom, Y., Schmandt, B., Polyak, V., DuFrane, S.A., 2010. Shrinking of the Colorado Plateau via lithospheric mantle erosion: evidence from Nd and Sr isotopes and geochronology of Neogene basalts. Geology 39, 27–30.

Crow, R., Karlstrom, K., Darling, A., Crossey, L., Polyak, V., Granger, D., Asmerom, Y., Schmandt, B., 2014. Steady incision of Grand Canyon at the million year timeframe: a case for mantle-driven differential uplift. Earth Planet. Sci. Lett. 397, 159–173.

DeCelles, P.G., 2004. Late Jurassic to Eocene evolution of the Cordilleran thrust belt and foreland basin system, western U.S.A. Am. J. Sci. 304, 105–168.

Dickinson, W.R., 1989. Tectonic setting of Arizona through geologic time. In: Jenney, J.P., Reynolds, S.J. (Eds.), Geologic Evolution of Arizona. Tuscon. In: Ariz. Geol. Soc. Dig., vol. 17, pp. 1–16.

Ducea, M.N., Saleeby, J.B., 1996. Buoyancy sources for a large, unrooted mountain range, the Sierra Nevada, California: evidence from xenolith thermobarometry. J. Geophys. Res. 101, 8229–8244.

Ducea, M.N., Kidder, S., Chesley, J.T., Saleeby, J.B., 2009. Tectonic underplating of trench sediments beneath magmatic arcs: the central California example. Int. Geol. Rev. 51, 1–26.

Ducea, M.N., Saleeby, J.B., Bergantz, G., 2015. The architecture, chemistry, and evolution of continental magmatic arcs. Annu. Rev. Earth Planet. Sci. 43, 299–331.

Dueker, K.G., Sheehan, A.F., 1997. Mantle discontinuity structure from midpoint stacks of converted P to S waves across the Yellowstone hotspot track. J. Geophys. Res. 102, 8313–8327.

Ellis, D.J., Green, D.H., 1979. An experimental study of the effect of Ca upon garnet–clinopyroxene Fe–Mg exchange equilibria. Contrib. Mineral. Petrol. 71, 13–22.

Esperança, S., Carlson, R.W., Shirey, S.B., 1988. Lower crustal evolution under central Arizona: Sr, Nd and Pb isotopic and geochemical evidence from the mafic xenoliths of Camp Creek. Earth Planet. Sci. Lett. 90, 26–40.

Flowers, R.M., 2010. The enigmatic rise of the Colorado Plateau. Geology 38, 671–672.

Flowers, R., Farley, K., 2012. Apatite $^4He/^3He$ and (U–Th)/He evidence for an ancient Grand Canyon. Science 338, 1616–1619.

Frost, B.R., Chamberlain, K.R., Schumacher, J.C., 2000. Sphene (titanite): phase relations and role as a geochronometer. Chem. Geol. 172, 131–148.

Hacker, B.R., Abers, G.A., 2004. Subduction factory 3: an Excel worksheet and macro for calculating the densities, seismic wave speeds, and H_2O contents of minerals and rocks at pressure and temperature. Geochem. Geophys. Geosyst. 5.

Henry, C.D., Hinz, N.H., Faulds, J.E., Colgan, J.P., John, D.A., Brooks, E.R., Cassel, E.J., Garside, L.J., Davis, D.A., Castor, S.B., 2012. Eocene–Early Miocene paleotopography of the Sierra Nevada–Great Basin–Nevadaplano based on widespread ashflow tuffs and paleovalleys. Geosphere 8, 1–27.

Horton, T.W., Chamberlain, C.P., 2006. Stable isotopic evidence for Neogene surface downdrop in the central Basin and Range Province. Bull. Geol. Soc. Am. 118, 475–490.

Humphreys, E., 1995. Post-Laramide removal of the Farallon slab, western United States. Geology 23, 987–990.

Huntington, K.W., Wernicke, B.P., Eiler, J.M., 2010. Influence of climate change and uplift on Colorado Plateau paleotemperatures from carbonate clumped isotope thermometry. Tectonics 29, 1–19.

Jiang, H., Lee, C.-T.A., Morgan, J.K., Ross, C.H., 2015. Geochemistry and thermodynamics of an earthquake: a case study of pseudotachylites within mylonitic granitoid. Earth Planet. Sci. Lett. 430, 235–248.

Johnson, C.M., 1990. Comment on "Lower crustal evolution under central Arizona: Sr, Nd and Pb isotopic and geochemical evidence from the mafic xenoliths of Camp Creek". In: Esperanca, S., Carlson, R.W., Shirey, S.B. (Eds.), Earth Planet. Sci. Lett. 99, 400–405.

Karlstrom, K.E., Lee, J.P., Kelley, S.A., Crow, R.S., Crossey, L.J., Young, R.A., Lazear, G., Beard, S.L., Ricketts, J.W., Fox, M., Shuster, D.L., 2014. Formation of the Grand Canyon 5 to 6 million years ago through integration of older palaeocanyons. Nat. Geosci. 7, 239–244.

Krieger, M.H., Creasey, S.C., Marvin, R.F., 1971. Ages of some Tertiary andesitic and latitic volcanic rocks in the Prescott–Jerome area, north-central Arizona. U.S. Geol. Surv. Prof. Pap. 750-B, B157–B160.

Krogh, E.J., 1988. The garnet–clinopyroxene Fe–Mg geothermometer – a reinterpretation of existing experimental data. Contrib. Mineral. Petrol. 99, 44–48.

Krogh-Ravna, E.J., 2000. The garnet–clinopyroxene Fe^{2+}–Mg geothermometer: an updated calibration. J. Metamorph. Geol. 18, 211–219.

Lee, C.-T.A., 2003. Compositional variation of density and seismic velocities in natural peridotites at STP conditions: implications for seismic imaging of compositional heterogeneities in the upper mantle. J. Geophys. Res. 108, 2441.
Lee, C.T.A., 2014. Physics and chemistry of deep continental crust recycling. In: Treatise on Geochemistry, second edition. Elsevier Ltd., pp. 423–456.
Lee, C.-T.A., Cheng, X., Horodyskyj, U., 2006. The development and refinement of continental arcs by primary basaltic magmatism, garnet pyroxenite accumulation, basaltic recharge and delamination: insights from the Sierra Nevada, California. Contrib. Mineral. Petrol. 151, 222–242.
Lee, C.-T.A., Thurner, S., Paterson, S., Cao, W., 2015. The rise and fall of continental arcs: interplays between magmatism, uplift, weathering, and climate. Earth Planet. Sci. Lett. 425, 105–119.
Levander, A., Miller, M.S., 2012. Evolutionary aspects of lithosphere discontinuity structure in the Western U.S. Geochem. Geophys. Geosyst. 13, 1–22.
Levander, A., Schmandt, B., Miller, M.S., Liu, K., Karlstrom, K.E., Crow, R.S., Lee, C.-T.A., Humphreys, E.D., 2011. Continuing Colorado Plateau uplift by delamination-style convective lithospheric downwelling. Nature 472, 461–465.
Lipman, P.W., 1992. Magmatism in the Cordilleran United States; progress and problems. In: Burchfiel, B.C., Lipman, P.W., Zoback, M.L. (Eds.), The Cordilleran Orogen. Geological Society of America, Conterminous, US, pp. 481–514.
Liu, K., Levander, A., Niu, F., Miller, M.S., 2011. Imaging crustal and upper mantle structure beneath the Colorado Plateau using finite frequency Rayleigh wave tomography. Geochem. Geophys. Geosyst. 12, 1–24.
Luffi, P., Saleeby, J.B., Lee, C.-T.A., Ducea, M.N., 2009. Lithospheric mantle duplex beneath the central Mojave Desert revealed by xenoliths from Dish Hill, California. J. Geophys. Res. 114, B03202.
McQuarrie, N., Chase, C.G., 2000. Raising the Colorado Plateau. Geology 28, 91–94.
Moucha, R., Forte, A.M., Rowley, D.B., Mitrovica, J.X., Simmons, N.A., Grand, S.P., 2008. Mantle convection and the recent evolution of the Colorado Plateau and the Rio Grande Rift valley. Geology 36, 439.
Müntener, O., Kelemen, P.B., Grove, T.L., 2001. The role of H_2O during crystallization of primitive arc magmas under uppermost mantle conditions and genesis of igneous pyroxenites: an experimental study. Contrib. Mineral. Petrol. 141, 643–658.
Nealy, L.D., Sheridan, M.F., 1989. Post-Laramide volcanic rocks of Arizona and northern Sonora, Mexico, and their inclusions. In: Jenney, J.P., Reynolds, S.J. (Eds.), Geologic Evolution of Arizona, Tuscon. In: Ariz. Geol. Soc. Dig., vol. 17, pp. 609–647.
Paterson, S.R., Ducea, M.N., 2015. Arc magmatic tempos: gathering the evidence. Elements 11, 91–98.
Polyak, V., Hill, C., Asmerom, Y., 2008. Age and evolution of the Grand Canyon revealed by U–Pb dating of water table-type speleothems. Science 80 (319), 1377–1380.
Reid, M.R., Bouchet, R.A., Blichert-Toft, J., Levander, A., Liu, K., Miller, M.S., Ramos, F.C., 2012. Melting under the Colorado Plateau, USA. Geology 40, 387–390.
Richard, S., Reynolds, S., Spencer, J., Pearthree, P., 2002. DGM-17 Digital Graphics Files for the Geologic Map of Arizona, a representation of Arizona Geological Survey Map 35, v. 1.0.
Roy, M., Jordan, T.H., Pederson, J.L., 2009. Colorado Plateau magmatism and uplift by warming of heterogeneous lithosphere. Nature 459, 978–982.
Sahagian, D., Proussevitch, A., Carlson, W., 2002. Timing of Colorado Plateau uplift: initial constraints from vesicular basalt-derived paleoelevations. Geology 807–810.
Saleeby, J.B., 2003. Segmentation of the Laramide Slab – evidence from the southern Sierra Nevada region. Geol. Soc. Am. Bull. 115, 655–668.
Smith, D., 2013. Olivine thermometry and source constraints for mantle fragments in the Navajo Volcanic Field, Colorado Plateau, southwest United States: implications for the mantle wedge. Geochem. Geophys. Geosyst. 14, 693–711.
Smith, D., Arculus, R.J., Manchester, J.E., Tyner, G.N., 1994. Garnet–pyroxene–amphibole xenoliths from Chino Valley, Arizona, and implications for continental lithosphere below the Moho. J. Geophys. Res. 99, 683–696.
Thompson, G., Zoback, M., 1979. Regional geophysics of the Colorado Plateau. Tectonophysics 61, 149–181.
Wendlandt, E., Depaolo, D.J., Baldridge, W.S., 1993. Nd and Sr isotope chronostratigraphy of Colorado Plateau lithosphere: implications for magmatic and tectonic underplating of the continental crust. Earth Planet. Sci. Lett. 116, 23–43.
Wernicke, B., Clayton, R., Ducea, M.N., Jones, C.H., Park, S.K., Ruppert, S., Saleeby, J.B., Snow, J.K., Squires, L., Fliedner, M., Jiracek, G., Keller, R., Klemperer, S., Luetgert, J., Malin, P., Miller, K., Mooney, W., Oliver, H., Phinney, R., 1996. Origin of high mountains in the continents: the Southern Sierra Nevada. Science 80 (271), 190–193.
Zandt, G., Myers, S.C., Wallace, T.C., 1995. Crust and mantle structure across the Basin and Range–Colorado Plateau boundary at ^{37}N latitude and implications for Cenozoic extensional mechanism. J. Geophys. Res. 100, 10529–10548.